



Ancient genomes reveal over two thousand years of dingo population structure

Yassine Souilmi^{a,b,1,2} , Sally Wasef^{c,d,1,2} , Matthew P. Williams^{a,e} , Gabriel Conroy^{f,g} , Ido Bar^h , Pere Bover^{i,j} , Jackson Dann^k , Holly Heiniger^l , Bastien Llamas^{a,l,m,n} , Steven Ogbourne^e , Michael Archer^o , J. William O. Ballard^p , Elizabeth Reed^q , Raymond Tobler^{a,r} , Loukas Koungoulos^{s,t,u} , Keryn Walshe^v , Joanne L. Wright^w , Jane Balme^x , Sue O'Connor^{s,u} , Alan Cooper^{y,1,2} , and Kieren J. Mitchell^{l,z,1,2}

Affiliations are included on p. 11.

Edited by Marcus Feldman, Stanford University, Stanford, CA; received April 17, 2024; accepted June 4, 2024

Dingoes are culturally and ecologically important free-living canids whose ancestors arrived in Australia over 3,000 B.P., likely transported by seafaring people. However, the early history of dingoes in Australia—including the number of founding populations and their routes of introduction—remains uncertain. This uncertainty arises partly from the complex and poorly understood relationship between modern dingoes and New Guinea singing dogs, and suspicions that post-Colonial hybridization has introduced recent domestic dog ancestry into the genomes of many wild dingo populations. In this study, we analyzed genome-wide data from nine ancient dingo specimens ranging in age from 400 to 2,746 y old, predating the introduction of domestic dogs to Australia by European colonists. We uncovered evidence that the continent-wide population structure observed in modern dingo populations had already emerged several thousand years ago. We also detected excess allele sharing between New Guinea singing dogs and ancient dingoes from coastal New South Wales (NSW) compared to ancient dingoes from southern Australia, irrespective of any post-Colonial hybrid ancestry in the genomes of modern individuals. Our results are consistent with several demographic scenarios, including a scenario where the ancestry of dingoes from the east coast of Australia results from at least two waves of migration from source populations with varying affinities to New Guinea singing dogs. We also contribute to the growing body of evidence that modern dingoes derive little genomic ancestry from post-Colonial hybridization with other domestic dog lineages, instead descending primarily from ancient canids introduced to Sahul thousands of years ago.

ancient DNA | dingo | Oceania | Palaeogenomics | domestication

Modern dingoes are free-living, naturalized canids that are found across most of mainland Australia and some nearby islands, including K'gari (known as Fraser Island from ~1840s to 2023; K'gari reinstated in 2023) (1). Between the arrival of their ancestors in Australia at least 3,000 B.P. (2) and the introduction of domestic dog breeds as part of European colonization, beginning in the 18th century, dingoes were isolated from domesticated dogs for thousands of years and represent an early “protodog” type lineage, divergent from other free-ranging and modern domestic dog representatives. Their early divergence and free-living status mean that dingoes were not subjected to the same intensive selective breeding as the ancestors of modern domestic breed dogs (3–5). Consequently, dingoes are behaviorally, genetically, and anatomically distinct from domestic dogs (3, 6–11) and—as the largest and most widespread terrestrial predator on the continent—they influence the distribution and abundance of many other animal species (12, 13) [though their impacts on ecosystem structure and function are debated (14)]. Further, dingoes play an important role in the lives and cultural heritage of many of Australia's Indigenous peoples (15), featuring prominently in their stories and spiritual beliefs (16) and occasionally being buried in the same manner as community members (17). However, despite recognition of their ecological and cultural importance, significant gaps persist in our understanding of dingo origins and evolution, particularly with respect to the extent of their recent hybridization with domestic dogs (9, 10, 18) and the impact of human activities on their behavior, distribution, and population structure (19).

Dingoes vary in appearance, size, and proportions across their range, suggesting the existence of distinct locally adapted dingo populations (1). Indeed, 3D geometric morphometrics analyses of dingo crania have shown that dingoes from southeastern Australia [namely Victoria, coastal New South Wales (NSW), and southern parts of mainland Queensland (QLD)] have overall smaller stature and reduced dental proportions compared to dingoes from further

Significance

Dingoes are an iconic element of Australia's biodiversity, but evidence-based management and conservation of dingoes depend on understanding their origins and population history. In this study, we present genomic data from ancient dingo individuals, providing a window into the early history of dingoes in Australia, prior to the introduction of modern domestic dogs and persecution of dingoes by European colonizers. Our results provide insights into the ancestry and origins of modern dingo populations, including their relationship to New Guinea singing dogs, and represent a valuable resource for future developments in dingo management and conservation.

Author contributions: Y.S., S.W., G.C., B.L., J.L.W., S.O., A.C., and K.J.M. designed research; Y.S. and S.W. performed research; G.C., S.O., M.A., J.W.O.B., E.R., L.K., K.W., J.L.W., J.B., S.O.C., and A.C. provided resources (samples); S.W., P.B., H.H., J.L.W., and K.J.M. performed DNA laboratory work; Y.S., S.W., M.P.W., I.B., J.D., R.T., and K.J.M. analyzed data; and Y.S., S.W., M.P.W., G.C., P.B., H.H., M.A., J.W.O.B., E.R., L.K., K.W., J.L.W., J.B., S.O.C., A.C., and K.J.M. wrote the paper.

The authors declare no competing interest.

This article is a PNAS Direct Submission.

Copyright © 2024 the Author(s). Published by PNAS. This article is distributed under [Creative Commons Attribution-NonCommercial-NoDerivatives License 4.0 \(CC BY-NC-ND\)](https://creativecommons.org/licenses/by-nc-nd/4.0/).

Although PNAS asks authors to adhere to United Nations naming conventions for maps (<https://www.un.org/geospatial/mapsgeo>), our policy is to publish maps as provided by the authors.

¹Y.S., S.W., A.C., and K.J.M. contributed equally to this work.

²To whom correspondence may be addressed. Email: yassine.souilmi@adelaide.edu.au, sally.wasef@qut.edu.au, alacooper@csu.edu.au, or kieren.j.mitchell@gmail.com.

This article contains supporting information online at <https://www.pnas.org/lookup/suppl/doi:10.1073/pnas.2407584121/-DCSupplemental>.

Published July 8, 2024.

north and west (including Western Australia, the Northern Territory, South Australia, and inland areas of NSW and QLD) (20, 21). This spatial pattern agrees with the results of genetic studies, which have also demonstrated that dingoes from southeastern Australia are distinct from other dingoes across the rest of mainland Australia. For example, dingo mtDNA haplotypes form two clades with geographically exclusive distributions—one clade is observed in dingoes from the southeast of Australia (and K'gari), while the other is observed in dingoes from across the rest of the country. Y chromosome haplotype frequencies and nuclear allele frequencies support the division of dingo diversity into these two main populations, though with finer-scale local structure within each population (22). The differences observed between dingoes across Australia have been interpreted by some authors as evidence that dingoes descended from at least two distinct source populations that were independently introduced to Australia, though it is probable there are other independent natural processes that have contributed, at least partly, to this differentiation as dingoes dispersed throughout the continent. It is also possible that the differences in the diversity and distribution of dingoes have been influenced by humans—particularly the persecution of dingoes by European settlers, ongoing lethal control of dingoes in most jurisdictions, and, in the mid-1900s, erection of a >5,000-km-long exclusion-fence to protect livestock interests in the state of South Australia.

Genetic research has also revealed intriguing similarities between dingoes and New Guinea singing dogs—endangered free-living dogs found in the highlands of New Guinea that bear a phenotypic resemblance to dingoes (23). A close genetic relationship between these two free-living canids has been acknowledged for some time (24), but more recent research has suggested that some dingoes share a relatively greater genetic affinity for New Guinea singing dogs (4, 6, 7, 22). Specifically, New Guinea singing dog mitochondrial haplotypes appear to be more closely related to dingoes from southeastern Australian and K'gari (the southeast mtDNA lineage) compared to other dingoes (4). This relationship is supported by genome-wide single nucleotide polymorphism (SNPs) (4, 25), though New Guinea singing dog Y chromosome haplotypes are more closely related to haplotypes at higher frequencies in the northwest dingo population (26). Broadly speaking, these genetic results are consistent with some morphological similarities between southeastern dingoes and New Guinea singing dogs, namely reduced dental proportions and smaller overall size (20, 21). Clearly, understanding the relationship between dingoes and New Guinea singing dogs is crucial for identifying the origins of both these canids, and the route and number of introductions of dogs to Australia during the Holocene. However, one obstacle to answering this question is uncertainty about the timing of gene flow between dingoes and New Guinea singing dogs. It is currently impossible to say whether gene-flow pre- or postdates the arrival of dingoes in Australia, and therefore whether the gene flow likely occurred in Island Southeast Asia or New Guinea, or in Australia itself.

In addition to questions surrounding the origin of dingo population structure and their relationship to New Guinea singing dogs, the extent to which dingoes have hybridized with other domestic dogs is also a topic of ongoing debate, with significant implications for dingo conservation and management (27). Pioneering genetic studies used a microsatellite assay to test for dingoes with hybrid ancestry (28, 29) with some follow-up studies using this technique concluding that domestic dog breeds—imported to Australia from the rest of the world since the 18th century—had hybridized extensively with dingoes and that domestic dog ancestry was prevalent in many modern dingo populations (30–32). Specifically, Stephens et al. (30) suggested that fewer than 1% of dingoes in southeast Australia were pure dingoes,

though Cairns et al. (31, 32) later revised this estimate to 18 to 41%. In contrast, a recent study based on genome-wide SNPs suggested that hybrid ancestry in modern dingoes is relatively rare, refuting the widespread existence of hybrids and “wild dogs” among dingo populations (22). However, all past studies on dingo ancestry have been based only on data from contemporary dingo populations, without an unequivocally “pure” baseline for dingo ancestry—this reduces the power of studies to detect pervasive hybrid ancestry and increases the risk of a circularity of reasoning.

Paleogenomic data from ancient, pre-Colonial dingo species could answer many of the outstanding questions about dingo origins and evolution described above. By providing a snapshot of genetic diversity at different points in dingo history, these data could establish a minimum age for events like gene flow between New Guinea singing dogs and dingoes, and the establishment of dingo population structure. Further, pre-Colonial dingoes should be free of any hybrid ancestry from modern domestic dog breeds, and could therefore serve as a baseline for validating the genomic purity of present-day dingo populations. Such paleogenomic data for dingoes are not yet available, likely due to the generally poor conditions for DNA preservation across most of mainland Australia. However, advances in high-throughput DNA sequencing technology have made paleogenomic studies of Australian fauna increasingly feasible (33–36).

In this study, we sequenced genetic data from 42 dingo specimens from coastal western Australia, the Nullarbor Plain, and coastal eastern Australia, spanning an east-west distance of over 3,000 km. The majority of dingo specimens we analyzed predate the arrival of Europeans in Australia—with several over 2,000 y old—and therefore represent the true genetic diversity of dingoes prior to any admixture with modern domestic dog breeds. Several specimens are from an archaeological context (17), including one specimen from coastal NSW that exhibited reduced stature and dental proportions—traits that link modern and ancient southeastern dingoes with New Guinea singing dogs, and differentiate them from dingoes to the west and north (20). We compared our ancient dingo genetic data to data from three modern dingoes from K'gari (an island-bound population thought to have minimal breed dog ancestry) and previously published data from other modern dingoes from across Australia (5), New Guinea singing dogs (5, 37), and modern and ancient dogs from the rest of the world (3, 37, 38). We used our ancient genetic data to test whether the geographic distribution of genetic diversity in ancient dingoes matches modern dingo population structure (implying local continuity of ancestry) and to compare models for dingo and New Guinea singing dog origins and population history. Finally, we used our ancient dingo genomes as a baseline to re-estimate the amount of dingo ancestry (versus post-Colonial breed dog ancestry) in a selection of modern dingoes that had previously been identified as pure dingoes using an established microsatellite assay, including several dingoes from K'gari.

Results

Ancient Genomes. DNA was extracted from 42 ancient dingo specimens (Dataset S1), but not all specimens yielded sufficient dingo sequences for downstream analysis. The final dataset comprises A) newly sequenced mtDNA data from 16 ancient dingoes, and $\geq 0.01\times$ mean depth-of-coverage nuclear genomic data from nine ancient dingoes (Fig. 1; two samples from the Nullarbor, one sample from southwest Western Australia, and six samples from coastal NSW); B) new mtDNA and nuclear genomic data from three present-day K'gari dingoes; and C)

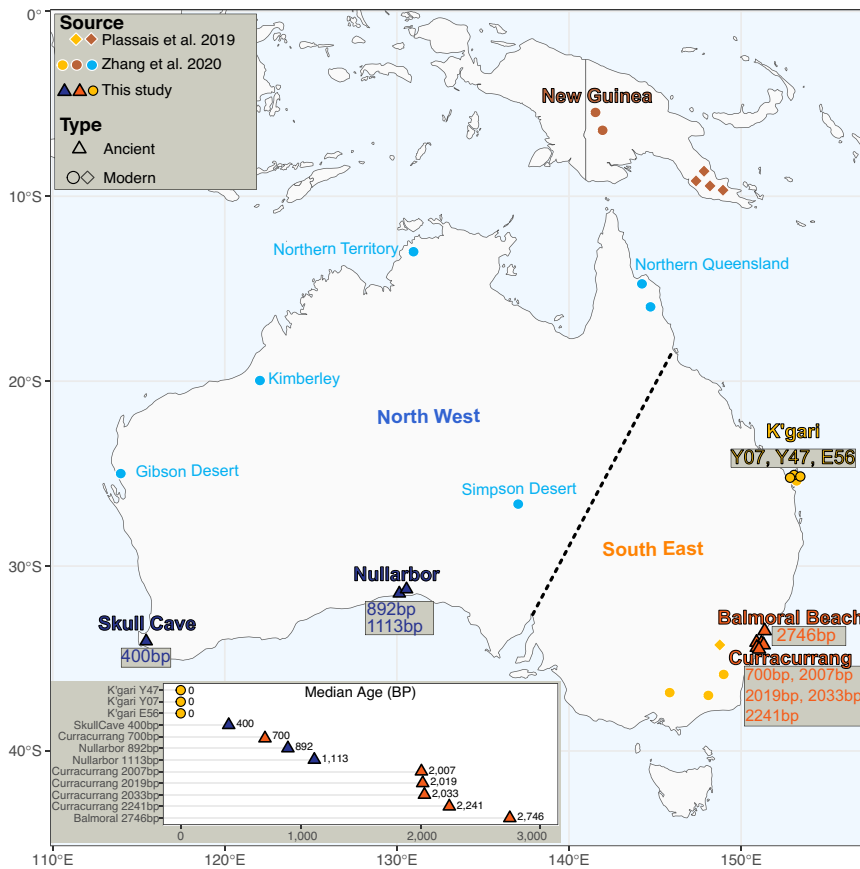


Fig. 1. Geographic and temporal distribution of dingo samples. Approximate locations of the modern and ancient dingo samples (labeled with lab ID numbers; see [Dataset S1](#)) with new genome-scale data presented in this study are shown on the map (ancient dingoes = blue and orange triangles, modern K'gari dingoes = bordered yellow circles). Yellow, blue, and red circles and diamonds (without black borders) represent the source localities for previously published data (5, 37, 39) from modern dingoes and New Guinea singing dogs. Broadly, dingoes are divided into two major populations in the “north west” (the blue shades) and the “south east” (orange/yellow); the dotted line roughly indicates the transition between these two populations (based on data from mtDNA, Y chromosome haplotypes, genome-wide SNPs, morphometric data, and environmental barriers). (*Inset*) estimated age of samples (median; years B.P./cal. years B.P.) for which new genome-scale data are presented in this study ([Dataset S1](#)).

previously published mtDNA and nuclear genomic data from modern dingoes, New Guinea singing dogs, and other domestic dogs from Southeast Asia and around the world.

Most notably, the new data included 16.6× and 2.83× mean depth-of-coverage genomic data from ancient dingoes from the Nullarbor (median ages = 892 and 1113 cal. years B.P., respectively; samples Nullarbor 892 bp and Nullarbor 1113 bp, respectively) and a 2.55× and 0.75× mean depth-of-coverage genome from ancient dingoes from Curracurrang in NSW (median ages = 2,019 and 2,007 cal. years B.P., respectively; samples Curracurrang 2019 bp and Curracurrang 2007 bp, respectively). In downstream statistical analyses, we used the highest depth-of-coverage genomes from the Nullarbor (Nullarbor 892 bp and Nullarbor 1,113 bp combined, labeled “Nullarbor”) and coastal NSW (Curracurrang 2019 bp and Curracurrang 2007 bp, labeled “Curracurrang 2k”) as exemplars of ancient dingo populations from western and eastern Australia, respectively, unless otherwise specified.

Mitochondrial DNA Analyses. Sixteen of our 42 ancient dingo specimens had both a direct radiocarbon age and more than 1,000 unique reads mapping to the mitochondrial reference sequence (the MT scaffold from the canFam3.1 genome assembly). Consensus sequences for these 16 dingoes, 10 modern dingoes, two New Guinea singing dogs, and one village dog from Bali were aligned with 33 previously published mitochondrial genome sequences downloaded from GenBank (total $n = 62$; [SI Appendix, Fig. S1](#)). A median-joining haplotype network created from this alignment grouped all modern and ancient dingoes into two clusters (Fig. 2): A) a cluster that contained dingoes from the modern northwest dingo mtDNA lineage and ancient dingoes from the Nullarbor; and B) a cluster that contained dingoes from the modern southeast dingo mtDNA lineage, ancient dingoes from Curracurrang, and two New Guinea singing dogs. Haplotypes from one additional

New Guinea singing dog and three other domestic dogs branched from a point in the network between the two clusters of dingo haplotypes. The monophyly of clusters A and B was strongly supported in our BEAST analysis (Bayesian posterior probability = 1.0 and 0.99, respectively; [SI Appendix, Fig. S1](#)), indicating that they were exclusive of each other and the remaining samples (three domestic dogs and one New Guinea singing dog). The 95% highest posterior density (95% HPD) for the time to most recent common ancestor (TMRCA) of cluster B was 3,424 to 8,244 B.P. (mean = 6,018) while the 95% HPD for the TMRCA of cluster A was 2,856 to 7,944 B.P. (mean = 5,480). Interestingly, two New Guinea singing dogs (genomic data from which are also analyzed in this study) share a haplotype that forms part of the same clade as ancient and modern dingoes from the east coast of Australia, whereas another New Guinea singing dog haplotype (a mtDNA sequence downloaded from GenBank: JX088674) shares an older and more distantly related common ancestor ([SI Appendix, Fig. S1](#)).

A Complex Population History. Within the broader spectrum of dog genetic diversity, the nuclear genomic ancestry and affinities of ancient dingoes are broadly similar to modern dingoes and New Guinea singing dogs (Fig. 3 and [SI Appendix, Figs. S3–S6](#)). In our Principal Component Analysis (PCA) (Fig. 3), PC1 (the x -axis) primarily reflected variation separating worldwide domestic dogs from a cluster of samples comprising dingoes (modern & ancient) and New Guinea singing dogs. In contrast, PC2 (the y -axis) primarily reflected variation within worldwide domestic dogs, though dingoes and New Guinea singing dog samples also exhibited some variation on PC2. Within our ancient dingoes, hierarchical clustering of log-transformed qpWave P -values ([SI Appendix, Fig. S6](#)) confirmed that our two highest depth-of-coverage ancient dingoes from the Nullarbor (Nullarbor 892 bp and Nullarbor 1113 bp) were closely related, as were our

two highest depth-of-coverage ancient dingoes from coastal NSW (Curracurrang 2019 bp and Curracurrang 2007 bp)—we combined data from these sample pairs in some downstream analyses to increase the amount of data representing each ancient population, unless otherwise stated.

We used f_4 -statistics to test whether other dingo and dog samples were symmetrically related to ancient dingoes from the Nullarbor (specifically Nullarbor 892 bp and Nullarbor 1113 bp, together labeled Nullarbor) and coastal NSW (specifically Curracurrang 2019 bp and Curracurrang 2007 bp, together labeled Curracurrang 2k) or shared more genetic drift—i.e., more shared ancestry—with one or the other population (Fig. 4 A, B, and D and *SI Appendix*, Fig. S5). Our results show that modern dingoes from K'gari and northern QLD appeared to have a significantly greater affinity to ancient dingoes from coastal NSW compared to ancient dingoes from the Nullarbor; modern dingoes from the Gibson Desert and Kimberley appeared to have a significantly greater affinity for ancient dingoes from the Nullarbor; and modern dingoes from the Northern Territory and Simpson Desert appeared to be symmetrically related to ancient dingoes from coastal NSW and the Nullarbor (or at least did not have a significantly greater affinity to one or the other). To simultaneously visualize the affinities of individual dingoes to ancient dingoes from the Nullarbor, and coastal NSW, and New Guinea singing dogs, we created a ternary plot where the three axes represented: 1) shared drift with Nullarbor 892 bp (the ancient Nullarbor dingo with highest depth-of-coverage), 2) shared drift with Curracurrang 2019 bp (the ancient coastal NSW dingo with highest depth-of-coverage), and 3) shared drift with a combination of data from all New Guinea singing dog individuals. Overall, Curracurrang 2007 bp, Curracurrang 2033 bp, and Curracurrang 700 bp had the greatest affinity to Curracurrang 2019 bp compared to all other dingoes; Nullarbor 1113 bp, Gibson Desert, and the Kimberley had the greatest affinity to Nullarbor 892 bp compared to all other dingoes (Fig. 4D).

While modern dingo individuals have a strong affinity for one or the other ancient dingo population, or neither, our admixture f_3 -statistic test results suggest that no modern dingo genome comprises a mixture of ancestry from the two populations represented by the ancient Nullarbor and Curracurrang genomes (Fig. 4C). However, we note that in the presence of substantial genetic drift in modern dingo populations, as would be experienced through extended bottlenecks, an admixture signature would be eroded and lead to a false negative result (40, 41). In addition, unequal contributions from the two ancient dingo populations with values close to the boundaries (0,1), and/or a short period between the split of the ancient dingo populations and the time of admixture, can further contribute to the erosion of the admixture signal (40, 41). Thus, additional genomes closing the temporal gap between modern and ancient Nullarbor and Curracurrang groups would be required to validate these findings.

While the ancient dingo groups are more closely related to each other than either is to modern New Guinea singing dogs (Fig. 4A and *SI Appendix*, Fig. S6), they do display asymmetry in their affinity to New Guinea singing dogs, with ancient dingoes from coastal NSW appearing to have a stronger affinity for New Guinea singing dogs compared to ancient and modern dingoes from South Australia and Western Australia (Fig. 4 B and D and *SI Appendix*, Fig. S6). Overall, Curracurrang 2033 bp, Curracurrang 700 bp, and modern alpine dingoes (from Victoria and southern NSW) have the greatest affinity to New Guinea singing dogs compared to all other dingoes (Fig. 4D). Using our ancient genomes (which are free of any confounding signal from domestic breed dog ancestry), we investigated demographic models that could explain varying levels of affinity for New Guinea singing dogs among different dingo populations: the most plausible scenarios (cf. Fig. 5 A and B) involve an initial split between the ancestral New Guinea singing dog population and an ancestral dingo population, followed by the establishment of distinct northwest dingo and southeast dingo populations, with gene flow occurring between

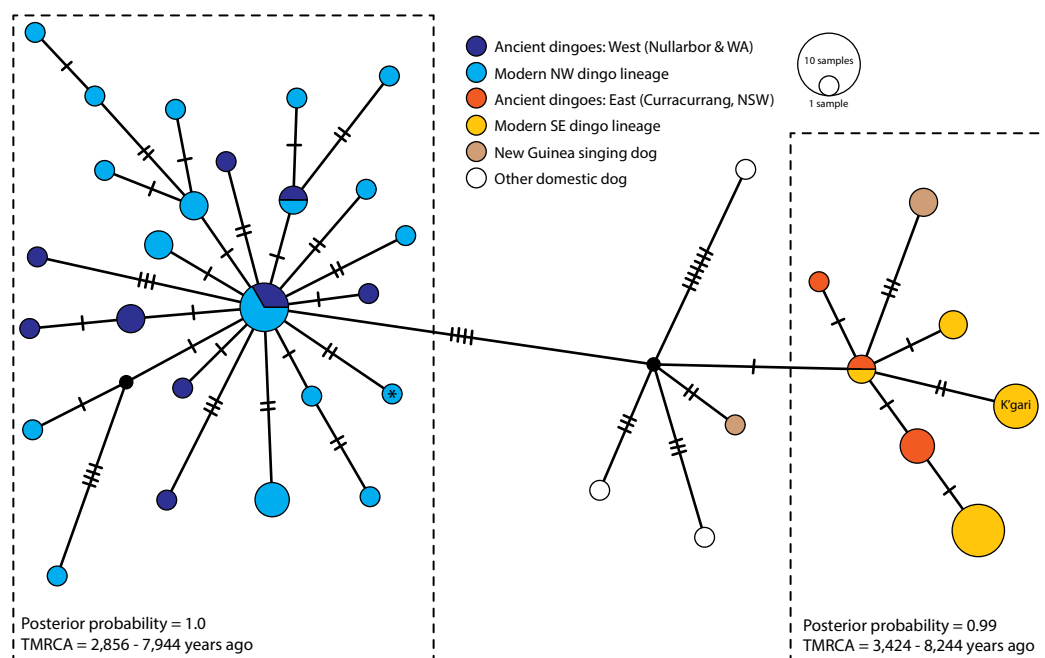


Fig. 2. Median-joining haplotype network of mtDNA from ancient dingoes, modern dingoes, New Guinea singing dogs, and other closely related domestic dog haplotypes (based on 69 segregating sites for which we had data for all 62 sequences). Each circle represents one haplotype, and the size of the circles is proportional to the number of samples. Haplotypes are colored dark blue for ancient dingoes from the Nullarbor and western WA, light blue for the modern northwest (NW) dingo lineage, dark orange for ancient dingoes from Curracurrang, light orange for the modern southeast (SE) dingo lineage, brown for New Guinea singing dogs, and white for other domestic dogs; black circles represent inferred (unobserved) intermediate haplotypes. Hatch marks along branches represent nucleotide substitutions separating haplotypes. The posterior probability and TMRCA (i.e., node age) we calculated using BEAST are presented for the two dingo clades (*SI Appendix*, Fig. S1). *This haplotype is part of the NW dingo lineage but belongs to an alpine dingo from Victoria, as originally observed by Cairns et al. (4); this may reflect natural or anthropogenic movement of a dingo individual or an accidental misattribution of sample metadata.

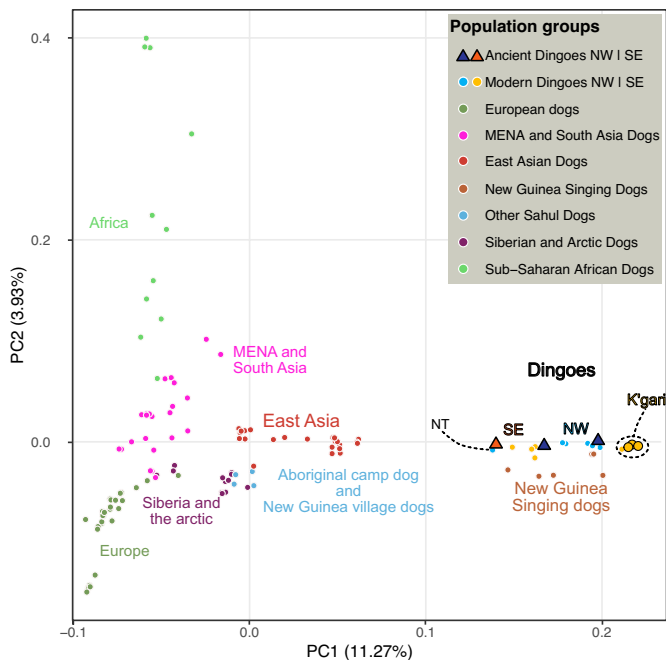


Fig. 3. PCA of nuclear genomic data from modern and ancient dingoes, New Guinea singing dogs, and worldwide diversity of other dogs (see *SI Appendix, Fig. S2* for a PCA including only dingoes, New Guinea singing dogs, and Asian village dogs; see *SI Appendix, Fig. S3* for a PCA expanded to include gray wolves). Samples with greater affinity to one another cluster together.

southeast dingoes and New Guinea singing dogs (Fig. 5 C and D). Gene flow may have been exclusively unidirectional from southeast dingoes into New Guinea singing dogs (Fig. 5C), exclusively

unidirectional from New Guinea singing dogs into southeast dingoes (Fig. 5D), or bidirectional between southeast dingoes and New Guinea singing dogs (impossible to model in qpGraph with available data). Given these results, we used DATES to estimate the putative timing of these admixture pulses, testing both possible directions of the gene flow (southeast dingoes into New Guinea singing dogs and New Guinea singing dogs into southeast dingoes; Fig. 6)—we estimated that admixture occurred around $2,456 \pm 171$ B.P. (assuming 3 y/generation and assuming that admixture occurred as a single pulse).

A Pre-Colonial Baseline for Dingo Genomic Ancestry. Using our ancient dingoes as an unadmixed baseline (because they predate the introduction of domestic dogs by Europeans), we estimated the proportion of dingo ancestry (versus post-Colonial domestic dog ancestry) in the genomes of our three modern K’gari dingoes and 11 other modern dingoes from two previous studies (5, 39). Prior to the present study, 13 of these modern dingoes had already been subjected to a microsatellite assay, which revealed no evidence for ancestry from post-Colonial domestic dogs [i.e., no alleles “diagnostic of dog”, and lod scores >2 (42) or average 3Q scores >0.1 (43)]—as a result, genomic data from these dingoes allowed us to test whether established microsatellite assays (and by extension SNP-based assays that operate on the same basis) are accurately measuring ancestry derived from true pre-Colonial dingo populations. We found no evidence for recent domestic dog ancestry in the majority of modern dingo individuals we examined (Fig. 7)—the only exceptions are a modern dingo sample from the Gibson Desert and one alpine dingo sample from Victoria, which have detectable ancestry derived from recent admixture.

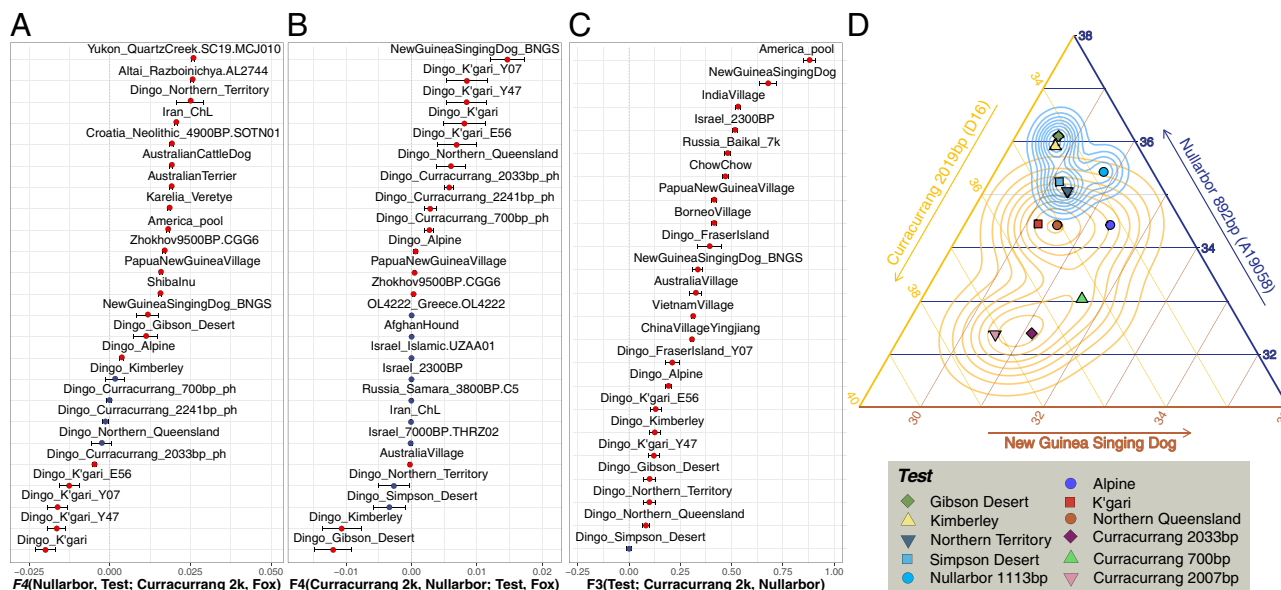


Fig. 4. Genetic affinities of ancient dingo clusters with modern and ancient canines. (A) Affinity f_4 -statistics of form f_4 (Nullarbor, *Test*; Curracurrang 2k, Andean Fox) where *Test* represents ancient and present-day canine groups (see *SI Appendix, Fig. S5A* for additional comparisons). Positive values indicate excess shared drift between Nullarbor and Curracurrang and/or between *Test* and an outgroup. Negative values indicate excess shared drift between *Test* and Curracurrang and/or between Nullarbor and an outgroup. (B) Symmetry f_4 -statistics were computed using f_4 (Curracurrang 2k, Nullarbor; *Test*, Andean Fox), where *Test* represents ancient and present-day canine groups (see *SI Appendix, Fig. S5B* for additional comparisons). Positive values indicate excess shared drift between Curracurrang and *Test* and/or between Nullarbor and an outgroup. Negative values indicate excess shared drift between Nullarbor and *Test* and/or between Curracurrang and an outgroup. The error bars represent two SE units, and the fill color indicates the statistical significance ($|Z| > 3$ in red). (C) Admixture f_3 -statistics in the form f_3 (*Test*; Curracurrang 2k, Nullarbor) where *Test* represents ancient and present-day canines. All observed values are positive, indicating that no *Test* group possesses allele frequencies that are consistent with being a mixture of the Curracurrang 2k and Nullarbor ancient dingo groups (see *SI Appendix, Fig. S5C* for additional comparisons). We document below multiple demographic processes that could be driving this signal, including those causing false negatives (40, 41). (D) Ternary plot showing the relative affinity of the *Test* populations (colored dots) to New Guinea singing dog (toward *Bottom Right*), Curracurrang 2019 bp (toward *Bottom Left*), and Nullarbor 892 bp (toward *Top*) respectively. Curracurrang 2007 bp, Curracurrang 2033 bp, and Curracurrang 700 bp had the greatest affinity to Curracurrang 2019 bp; Nullarbor 1113 bp, and modern dingoes from the Gibson Desert and the Kimberley had the greatest affinity to Nullarbor 892 bp; and Curracurrang 2033 bp, Curracurrang 700 bp, and modern alpine dingoes had the greatest affinity to New Guinea singing dogs compared to all other dingoes.

Discussion

Dingo Phylogeography, Population Structure, and Continuity of Ancestry. The results of our genomic and mtDNA analyses confirm that population structure had already emerged in dingo populations as early as 2,000 B.P. (our oldest ancient dingo samples), and since that time there has been some level of local continuity between ancient and modern dingo populations. Our results strongly support the inclusion of ancient dingo mtDNA haplotypes within the two previously recognized dingo mtDNA lineages (Fig. 2)—our ancient dingoes from coastal Western Australia and the Nullarbor are part of the modern NW dingo mtDNA lineage, while our ancient dingoes from coastal NSW are part of the modern SE dingo mtDNA lineage. Consistent with the results of previous studies (26, 44), we estimated that the common ancestor of each lineage (including our corresponding ancient samples) occurred between ~3,000 and ~8,000 B.P. (Fig. 2 and *SI Appendix, Fig. S1*), representing lower and upper bounds on the likely time frame for the introduction of dingoes to Australia and the beginning of their subsequent diversification and population expansion (2, 4, 45). However, because mtDNA is a single maternally inherited locus, it is susceptible to incomplete lineage sorting and other demographic biases. Consequently, we compared our mtDNA results to those obtained with our nuclear genomic dataset.

Our genomic analyses showed relationships between modern and ancient dingoes that were largely consistent with our mtDNA results (Fig. 4 *A* and *B*). While modern and ancient dingoes were

generally closely related (Fig. 3), ancient dingoes from the Nullarbor had a greater genomic affinity for modern dingoes from the Kimberley and the Gibson Desert. In contrast, ancient dingoes from coastal NSW had a greater affinity for modern dingoes from K'gari and mainland QLD. However, we cannot exclude the possibility that whole-genome enrichment of our ancient coastal NSW dingoes with probes based on K'gari dingo DNA resulted in an ascertainment bias that at least partly explains these results. Nevertheless, the geographic delineation of mtDNA haplotypes substantially predates the arrival of domestic dogs and post-Colonial anthropogenic persecution and influence on dingo populations. Finally, we found no evidence that any modern dingo group was formed as a mixture of ancestry from ancient dingoes from the Nullarbor and coastal NSW (Fig. 4C). However, multiple demographic conditions have been shown to increase the probability of false rejections, such as short periods between the split of the admixing sources and the formation of the admixed population, very small or large admixture proportions, and significant genetic drift in the admixed population post their formation, all of which are possible explanations for the relationship between ancient and modern dingoes (40, 41).

Ancient Dingo Genomes Are a Resource for Dingo Management and Conservation. We used f_4 statistics based on genome-wide SNPs to estimate the proportion of dingo ancestry in the genomes of 14 modern dingo individuals, 13 of which had previously been identified

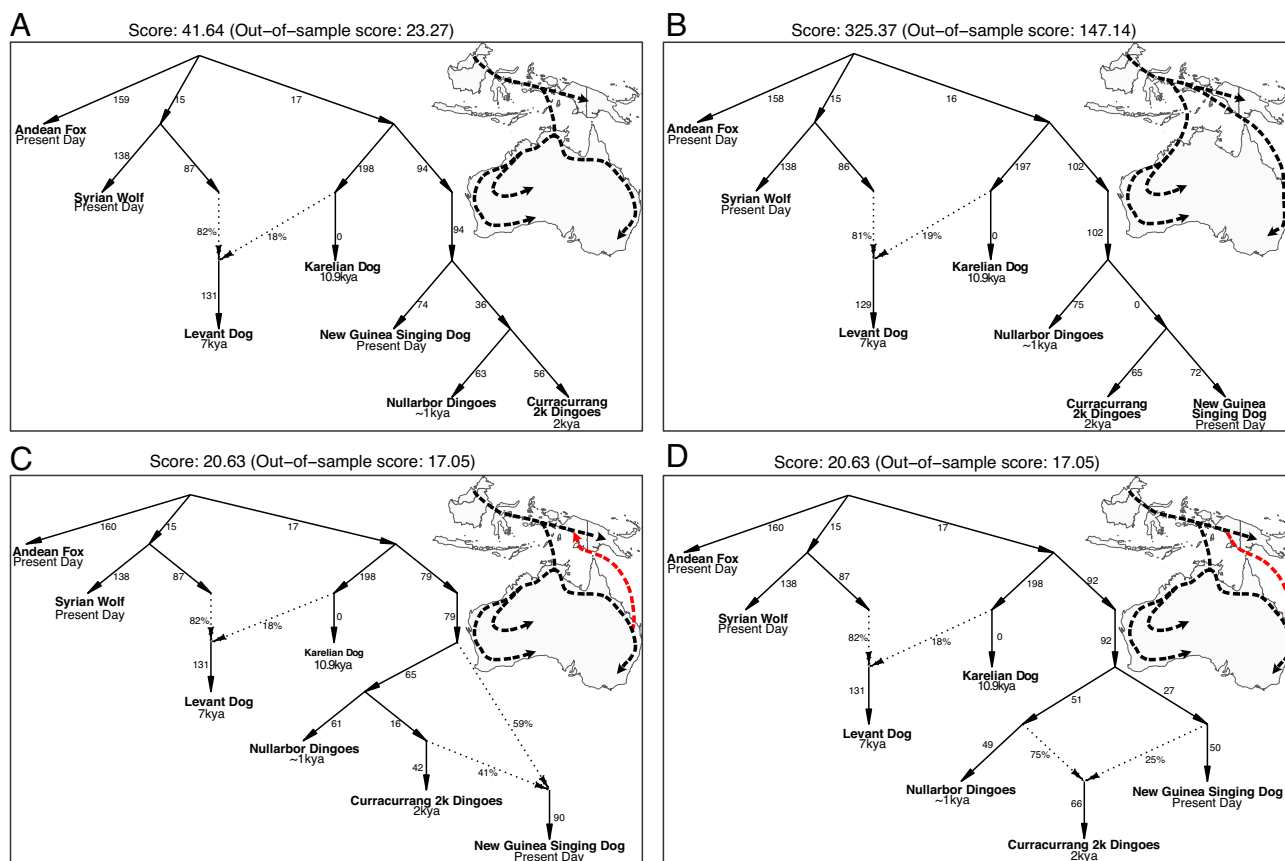


Fig. 5. Best fitting *qpGraph* models for relationships between ancient dingoes from the Nullarbor, ancient dingoes from coastal NSW, and modern New Guinea singing dogs (model framework based on best-fitting models for dog ancestry from Bergström et al.'s Fig. 4F (38)). (A) Represents a simple phylogenetic model. (B) Model that explains the excess affinity between coastal NSW dingoes and New Guinea singing dogs by a subsequent later split than eastern dingoes from the common ancestor. (C and D) Represent models that include admixture between dingoes and New Guinea singing dogs (*Bottom Left* and *Bottom Right*) fit better (i.e., lower likelihood score) than models without admixture (*Top Left* and *Top Right*); however, it is impossible to determine the direction of admixture with the available data (models are equally well-fitting; same likelihood score). The arrows and divergence points in the maps are indicative only, and should be treated as hypotheses for future research—our genomic data do not provide information about the geographical origins of lineages or their exact migration routes.

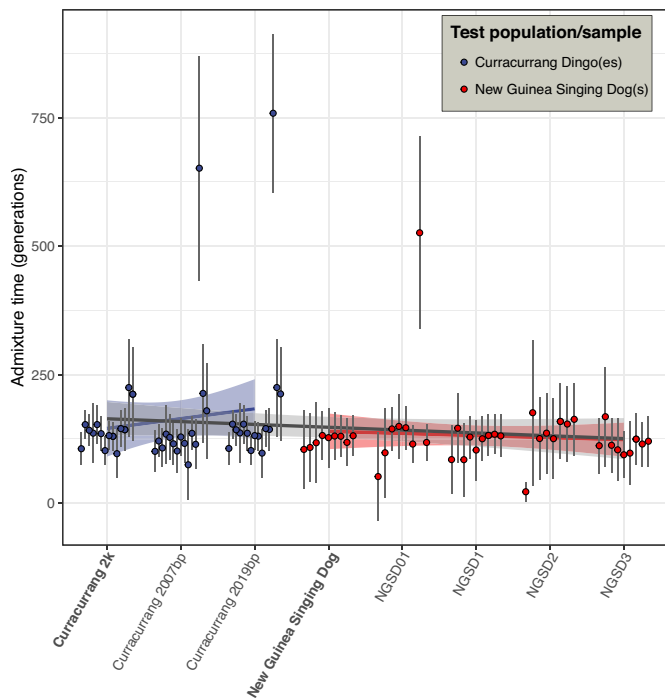


Fig. 6. Putative admixture time between the ancestors of ancient dingoes from coastal NSW and New Guinea Singing Dogs. The blue dots represent the estimates for gene flow from New Guinea singing dogs into dingoes represented by the Curracurrang 2k cluster, and the red dots represent estimates for gene flow from dingoes into New Guinea Singing Dogs. We replicated the estimate using all available Curracurrang dingoes and New Guinea Singing Dogs grouped as populations (bolded) and as individual samples (not all individuals or populations could be used in all comparisons due to a lack of overlapping loci for some of the ancient dingoes with lower average depth-of-coverage). The mean estimated admixture pulse time is 147.74 ± 57.03 generations before the oldest used sample included in the test, or $2,456 \pm 171$ B.P. assuming 3 y/generation .

as pure dingoes using a microsatellite assay. In our comparisons, most of these pure dingoes exhibited no evidence for post-Colonial dog ancestry (Fig. 7), confirming that no pervasive undetected admixture with post-Colonial dogs occurred in the lineage of these modern individuals. However, two samples previously identified as pure contained detectable (though minimal) levels of post-Colonial dog ancestry; this suggests that tests for hybridization might be underpowered when *a priori* pure dingoes—like our ancient pre-Colonial individuals—are not represented in comparative datasets. In addition, based on their analysis of genome-wide SNPs from modern dingoes, Cairns et al. (22) suggested that dingo population structure and biases in marker selection may cause microsatellite assays to underestimate the true proportion of dingo ancestry in dingo genomes (versus post-Colonial dog ancestry). Together, these results indicate that researchers and wildlife managers should treat the results of routine dingo microsatellite assays with caution. We emphasize that genetic tests for dingo “purity” need further refinement before they can reach their full potential robustness and usefulness; this refinement should include comparing a wider range of known hybrid individuals to genomic data from ancient dingoes. In this respect, our ancient dingo genomes represent a valuable resource for future developments in dingo management and conservation (27).

The Relationship between Dingoes and New Guinea Singing Dogs. While we cannot exclude that ascertainment bias from the whole genome enrichment accounts for some of the observed genomic affinity between ancient dingoes from coastal NSW and K’gari, it is notable that the New Guinea singing dog samples have the strongest signal of excess allele sharing with ancient

dingoes from coastal NSW (Fig. 4B). The latter signal cannot be explained just as an artifact caused by ascertainment bias, because: 1) the strength of the affinity between ancient dingoes from coastal NSW and New Guinea singing dogs exceeds that of the affinity between the former and dingoes from K’gari (Fig. 4 B and D), and 2) data from the New Guinea singing dogs and K’gari dingoes were obtained using shotgun sequencing (not whole genome enrichment). This result is particularly interesting because the ancient specimen from coastal NSW from which we have the highest depth-of-coverage genomic data (Curracurrang 2019 bp) exhibited reduced stature and dental proportions relative to modern dingoes from populations to the west and north—phenotypic characteristics shared with New Guinea singing dogs (20). Since our ancient dingoes—including Curracurrang 2019 bp—predate any post-Colonial admixture with domestic dogs, our results present a unique opportunity to explore the origin of previously reported signals for relatedness between modern dingoes from the southeast of Australia and New Guinea singing dogs (4, 7, 20, 21, 26).

Our demographic model testing shows that simple models for the relationship between present-day New Guinea singing dogs, ancient dingoes from the Nullarbor, and ancient dingoes from eastern NSW that do not include admixture between any of these populations are a relatively poor fit (Fig. 5 A and B). Models that allow for admixture between present-day New Guinea singing dogs and ancient dingoes from coastal NSW (Fig. 5 C and D) are a better fit, but our data do not allow us to test the overall directionality of gene flow—i.e., New Guinea singing dogs may possess ancestry from ancient dingoes, or some dingoes may derive ancestry from a population related to present-day New Guinea singing dogs. In either case, this signal appears to be consistent with an initial split between dingoes and New Guinea singing dogs followed by a secondary pulse of interbreeding between 2,285 and 2,627 B.P. (mean = 2,456 B.P.; Fig. 6). This timeframe aligns closely with our mean age estimate for the most recent common ancestor of mtDNA haplotypes from two New Guinea singing dogs and their nearest relatives in the SE dingo mtDNA lineage (2,472 B.P., 95% HPD = 765 to 4,611 B.P.; SI Appendix, Fig. S1). These dates are also broadly consistent with population separation ages estimated using the cross-coalescence rate between X chromosome haplotypes from pairs of modern dingoes and New Guinea singing dogs (SI Appendix, Figs. S7 and S8)—estimates of $\leq 2,500$ B.P. were obtained for many pairs, though there was high variability overall and estimates for several pairs were as old as $\sim 7,000$ B.P.

Several previous studies have concluded that deep splits between dingo mtDNA haplotypes and/or Y chromosome haplotypes—and the geographical distribution of these haplotypes—constitute evidence that dingoes descend from at least two populations that were independently introduced to Australia (4, 26) [contrary to some earlier assertions that dingoes descend from one population (24), or even introduction of a single pregnant female (46)]. Our results recapitulate these deep splits and allow us to enumerate several models for the timing and number of population movements. One scenario that is consistent with our results involves the introduction of at least two genetically distinct canid populations to Australia: one population from which western dingoes (including our ancient Nullarbor dingoes) derive almost all of their ancestry, and—perhaps more recently—another population that was closely related, but with a greater affinity to present-day New Guinea singing dogs. In this first scenario, gene flow between the ancestors of New Guinea singing dogs and dingoes occurred outside of Australia, perhaps reflecting ancient structure or differentiation within a shared ancestral population located somewhere in island southeast Asia. However, a scenario involving the

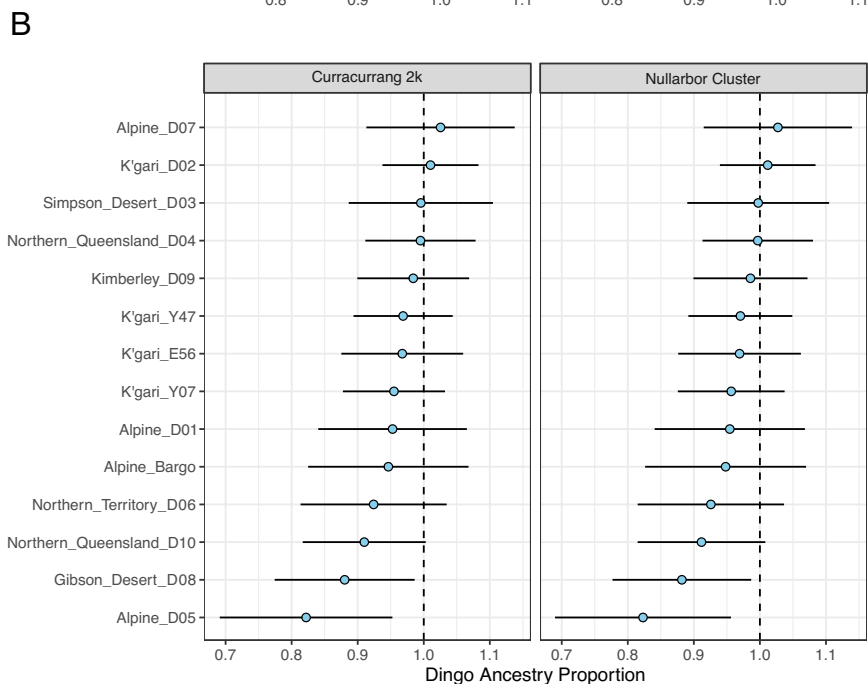
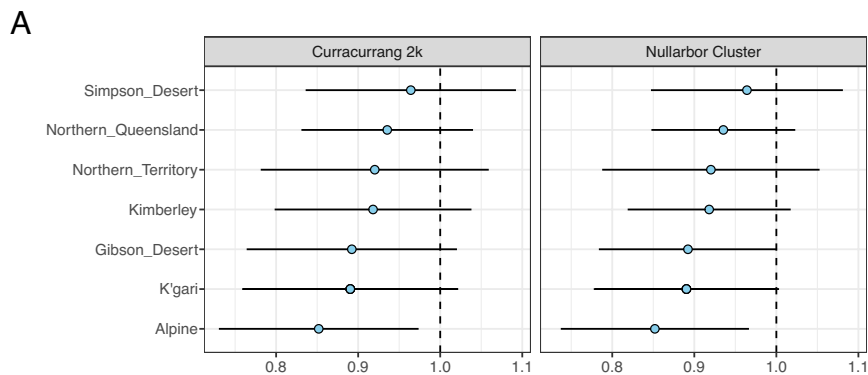


Fig. 7. Proportion of modern dingo genomes ancestry derived from a population represented by our ancient dingo genomes (as opposed to the genomes of breed dogs). These modern dingoes had previously been subjected to a microsatellite assay that uncovered no evidence for hybrid ancestry (i.e., they were presumed pure dingoes) with the exception of Alpine_Bargo, for which the level of dingo ancestry had not previously been tested. Ancient dingo ancestry is represented here by either Curracurrang 2k (*Left*) or Nullarbor (*Right*)—results are highly consistent regardless of which ancient dingo is used in the test. Ancestry proportion is represented by α (the f_2 ratio). (A) shows the aggregate α value for modern dingoes when grouped into populations, whereas panel (B) shows that there is variability between individuals within populations.

movement of New Guinea singing dog individuals to eastern Australia—and their subsequent absorption into the local dingo populations through interbreeding—could also explain our results. A final scenario involves the introduction of at least one ancestral dog population to Australia, which expanded and differentiated into locally distinct dingo populations, one of which (from eastern Australia) subsequently transmitted alleles to the population from which present-day New Guinea singing dogs are primarily derived. These scenarios are not mutually exclusive, and using our data we cannot exclude that recent gene flow between dingoes and New Guinea singing dogs was bidirectional.

The cessation of land connection between Australia and New Guinea by the early Holocene means that humans were almost certainly implicated in facilitating subsequent gene flow between ancient dingoes and New Guinea singing dogs, which may have occurred only in the last 3,000 y (Figs. 2 and 6 and *SI Appendix*, Figs. S1, S7, and S8). Despite a lack of evidence for gene flow between Indigenous Peoples from Australia and New Guinea throughout most of the Holocene (47), some authors have suggested that Aboriginal Australian Peoples from northern QLD share some cultural traits with other peoples from Near Oceania, including New Guinea and/or the Torres Strait Islands (48–51). Aboriginal Australian Peoples from northern QLD also appear to have been traveling between the mainland and offshore islands during the mid- to late Holocene (52). Finally, there is precedent for overwater movement of dingoes by Aboriginal Australian

Peoples—the Butchulla People, Traditional Owners of K'gari, facilitated movement of dingoes between K'gari and the mainland in pre-Colonial times (53). Together, these observations suggest the possibility of cultural interaction and trade, however limited, that may have provided a conduit for movement between Australia and New Guinea during the Holocene.

Conclusion. In this study, we demonstrate that modern dingoes inherit their population structure and the overwhelming majority of their ancestry from ancient dingo populations, which had already differentiated within Australia by ~2,000 B.P. Our new data from ancient dingoes, which predate post-Colonial hybridization between dingoes and other dogs, will be a valuable resource for future refinement of assays for determining dingo ancestry in conservation contexts. Finally, we contribute insights into the complicated relationship between dingoes and New Guinea singing dogs and highlight several models that may be tested by future studies. Validating these models will require genetic data from ancient dogs from northern Australia, island southeast Asia (e.g., Indonesia, Borneo, and/or the Philippines), and/or New Guinea, to reveal the extent of differentiation in the population(s) ancestral to dingoes and New Guinea singing dogs prior to (and immediately following) their arrival in Sahul. Long-term DNA preservation is relatively poor in hot and humid environments; however, the recent publication of genomic data from mid-Holocene human remains from Sulawesi (54) indicates that it is technically feasible to obtain data of the

necessary age and geographical origin to cast further light on the origin of dingoes—it may only be a matter of identifying suitable specimens.

Materials and Methods

Samples. We sampled 42 ancient dingo specimens (Dataset S1). Seven specimens were collected from archaeological sites in coastal NSW: Curracurrang Rockshelter and Balmoral Beach—the archaeological context of the Curracurrang Rockshelter specimens was described by Koungoulos et al. (17). Twenty seven specimens were collected from limestone caves on the Nullarbor Plain between 2016 and 2018 as part of paleontological fieldwork led by one of us (ER) with the assistance of members of the Australian Speleological Federation. Two additional specimens (a skull and an ulna) were collected from Koonalda Cave on the Nullarbor Plain in 2018 by Keryn Walshe with the assistance of Clem Lawrie (Senior Custodian and Native Title Holder). We also sampled six ancient dingoes from different sites in South Australia and Western Australia from the South Australian Museum and Western Australian Museum collections, respectively. To identify any background lab contamination and/or cross-contamination, negative (no template) controls were included alongside each batch of ancient dingo samples in all laboratory and analysis steps; we observed no evidence that contamination occurred at any step during our study.

To compare with our ancient dingoes, we obtained three K'gari dingo tissue (ear tag) samples that were collected by the QLD Parks and Wildlife Service (QPWS) as part of routine QPWS activities (in 2005, 2012, and 2014). Based on QPWS observations, these dingo individuals were not immediately related to one another, though the island's dingo population is small [~70 to 173 individuals (55, 56)]. Previous commercial analysis of these samples by Zoological Genetics (Adelaide, Australia) using the microsatellite assay established by Stephens (28) and Wilton et al. (29) indicated that all three individuals were pure dingoes [i.e., zero alleles diagnostic of dog ancestry; average 3Q scores >0.1 (43)]. We also downloaded previously published data from 11 other modern dingoes, six New Guinea singing dogs, and 372 other domestic dogs, wolves, and other canids (3, 5, 37–39, 57–62) (Datasets S2 and S3). The 10 modern dingoes from Zhang et al. (5) that we included in our dataset had also been subjected to a microsatellite assay (at the University of New South Wales)—this assay (performed as a service for Zhang et al. by an author of the present study, JWOB) suggested they were pure dingoes [i.e., zero alleles diagnostic of dog ancestry; lod scores >2 (42)]. The eleventh dingo from which we downloaded genomic data, published by Freedman et al. (39), had not previously been subjected to microsatellite testing as far as we are aware.

AMS radiocarbon dating was carried out on bone and tooth samples from 29 of the ancient dingo specimens (three at the Research School of Earth Sciences, Australian National University and 26 at the Oxford Radiocarbon Accelerator Unit, University of Oxford). Radiocarbon ages for five specimens were obtained from a published study (17). All ages were calibrated using OxCal (63) v4.4 with the Southern Hemisphere calibration curve SHCal20 (64) (Dataset S1).

Laboratory Work. DNA was extracted from 13 ancient dingo specimens at the Australian Research Centre for Human Evolution (ARCHE) at Griffith University. DNA was extracted from an additional 29 ancient dingo specimens at the Australian Centre for Ancient DNA (ACAD) at the University of Adelaide. DNA was extracted from the three modern K'gari dingo samples in the modern DNA laboratory at Griffith University. See *SI Appendix* for detailed DNA extraction methods.

DNA extracted from dingo samples at the ARCHE at Griffith University was subjected to Meyer and Kircher's (65) library preparation protocol with the addition of Rohland et al.'s (66) partial UDG treatment as described in Wasef et al. (33). DNA extracted from 27 of the dingo samples at the ACAD at the University of Adelaide was also subjected to Meyer and Kircher's (65) library preparation protocol (using truncated Illumina adapters) with the addition of Rohland et al.'s (66) partial UDG treatment and ligation of unique 7-mer 5' and 3' barcoded adapters during the ligation step. Additional libraries were created at ACAD from DNA extracted from two additional samples (ACAD19054 and ACAD19058) following the same protocol as described above but omitting the addition of Uracil Glycosylase Inhibitor (New England Biolabs), such that all uracils were removed, and using nonbarcoded adapters. Sequencing libraries were created from the DNA extracted from the three modern K'gari dingo samples using the Ultra II

kit (New England Biolabs) following the manufacturer's manual protocol. See *SI Appendix* for detailed library preparation methods.

Libraries created at ARCHE for six ancient dingoes underwent whole genome hybridization enrichment using modern domestic dog DNA (Dataset S1). The other seven ancient dingoes (Dataset S1) underwent whole genome hybridization enrichment using baits based on modern K'gari dingo genomic DNA. Libraries created at ACAD for two ancient dingoes (Dataset S1) underwent enrichment for mammal mitochondrial DNA following the protocol described by Mitchell et al. (67). See *SI Appendix* for detailed hybridization enrichment methods. Libraries created at ACAD for the remaining 27 ancient dingoes were not subject to hybridization enrichment, nor were the libraries created for the three modern dingoes from K'gari.

Enriched libraries from ancient samples created at ARCHE were sequenced on multiple lanes of an Illumina HiSeq 4000 (1 × 100 bp single-end) at The Danish National High-Throughput DNA Sequencing Centre in Copenhagen (for samples D2 to D8) or an Illumina HiSeq X (2 × 150 bp paired-end) by Macrogen (for samples D10 to D16). Libraries created at ACAD were sequenced across multiple flow cells on an Illumina NextSeq 500 (high-output mode, 2 × 75 bp paired-end) by the Australian Genome Research Facility (AGRF) and an Illumina HiSeq X (2 × 150 bp paired-end) by the Kinghorn Cancer Centre at the Garvan Institute of Medical Research. Pooled libraries from the three modern K'gari samples were sequenced on an Illumina HiSeq X (2 × 150 bp paired-end) by Novogene Bioinformatics Technology Corporation Limited in Beijing, China. See *SI Appendix* for detailed high-throughput DNA sequencing methods.

Ancient Genomic Data Processing & Quality Control. All ancient DNA sequencing data were processed using EAGER pipeline (68) v2.3.5 running with NextFlow (69) v21.04.2. In brief, AdapterRemoval (70) v2.3.1, was used to detect and trim adaptor sequences, followed by collapsing overlapping reads, after which we removed reads shorter than 20 bases. The remaining reads were aligned to the canFam3.1 reference genome using BWA (71) aln v0.7.17-r1188 (-n 0.01 -l 1024 -o 2), and we deduplicated the mapped reads using "MarkDuplicates.jar" in PicardTools v2.22.9 (<https://github.com/broadinstitute/picard>). Finally, we soft-clipped two bases from the mapped read termini using BamUtil trimBam (72) v1.0.14 to eliminate the impact of DNA damage on variant calling (uracils were enzymatically removed during library preparation, except at the terminal nucleotide in some libraries; Dataset S2).

To authenticate aDNA, we first used the DNA damage profile generated using DamageProfiler (73) v0.4.9. We further explored the impact of contamination on each library using angsd (74) v0.933, where the contamination levels are estimated by comparing the level of heterozygosity of chromosome X to the autosomes. We contrasted these results against the contamination levels on the mitochondrial genomes using the Calico package v0.2 (<https://github.com/pontusssk/calico>), where for each ancient genome, the minor alleles count to major alleles counts ratio is calculated, and the 95% CI is estimated by contrasting the results against a reference database.

Additionally, we used quality control and visualization tools in FastQC v0.11.9 (<https://www.bioinformatics.babraham.ac.uk/projects/fastqc/>) and fastP (75) v0.11.9 to check sequencing quality, duplication levels, overrepresented sequences, and detection of residual adapter/barcode content. Finally, we used endorS.py v0.4 (<https://github.com/aidaanva/endorS.py>), MTNucRatioCalculator v0.7 (<https://github.com/apeltzer/MTNucRatioCalculator>), Sex.DetERRmine (76) v1.1.2, and Qualimap (77) v2.2.2-dev to estimate the endogenous content for each library, calculate the mitochondrial to nuclear genome mapping ratio, assign genetic sex, and generate depth of coverage and other useful alignment quality metrics respectively.

Published Reference Datasets. We supplemented the dataset of ancient dingoes we are introducing here with 10 modern dingoes and two New Guinea singing dog whole-genome shotgun sequenced samples sourced from Zhang et al. (5) (Dataset S2). We processed the sequencing data from these samples using EAGER pipeline as well with the following differences: we did not collapse overlapping reads, we aligned the reads to the CanFam 3.1 reference genome using BWA MEM (v0.7.17-r1188) with default parameters, and did not perform any clipping of read termini.

In addition, we used publicly available genome-wide dataset of modern canids from Plassais et al. (37), obtained in VCF format, and ancient canids from Berström et al. (3, 38) (Dataset S3), who collated data from a number of earlier studies (3, 5, 37, 38, 57–62) in PACKEDANCESTRYMAP format provided by Anders

Bergström upon request. We explored the inclusion of SNP-array-based genotyping data from modern dingoes [e.g., Cairns et al. (25)]; however, ascertainment bias associated with the SNP array data mean they could not be compared with SNPs generated from our whole-genome datasets (SI Appendix, Fig. S9).

Variant Calling. As the confidence of de novo variant calls from ancient genomes is low, we adopted a similar SNP ascertainment process as the one used by Bergström et al. (38) where we start with the variable loci from the large Plassais et al. (37) dataset, and only retain transversion polymorphic loci in coyotes, a known outgroup with no evidence of admixture with any canid populations outside of North America (3, 38). We used SequenceTools pileupCaller (v1.14.0.5; <https://github.com/stschiff/sequenceTools>) to generate pseudohaploid calls, where a homozygote diploid call is created by sampling one random sequencing read (with a mapping quality threshold of 20) at each of the 19.1 million biallelic SNP loci retained, while controlling for the two alleles. For all further analyses, the genotype data was merged with a subset of the datasets from Plassais et al. (37) and Bergström et al. (3, 38).

Principal Component Analysis. We used a representative sample of worldwide canine diversity for this analysis in PACKEDANCESTRYMAP format with Eigensoft SmartPCA (78, 79) v16000 with newshrink, inbreed, and noxdata parameters turned on and the numoutlier parameter set to zero. We tested with and without projection (lsqproject) and found that in our case it made no substantial difference to the results. Final results were plotted using ggplot2 (80) and R (81) v4.3.0.

qpWave and Sample Clustering. We conducted hierarchical clustering on ancient dingo samples to form analysis groups and determine whether the geographical patterns observed in the mitochondrial genome are also present genome-wide. We generated a distance matrix based on $-\log_{10}$ transformed qpWave *P*-values where we performed pairwise analyses of dingo groups as the left set and specified a global reference set of 24 right groups building on Bergström et al. (3) to capture any unique ancestry among the ancient dingoes:

CoyoteCalifornia, Ireland_Neolithic.Newgrange, Sweden_Neolithic.C88, Sweden_BronzeAge.C62, Croatia_Eneolithic.ALPO01, Israel_7000BPTHRO2, Sweden_StoraForvar_4000BPC94,AL2397_Italy.AL2397,AL2946_Plocnik.AL2946,OL4029_Spain.OL4029,Karelia_Veretye,OL4222_Greece.OL4222,Israel_2300BP,Germany_LateNeolithic.CTC,Germany_7k,Croatia_Neolithic_4900BPSOTN01,Sweden_PWC,America_pool,Russia_Baikal_7k,Iran_ChL,Russia_Samara_3800BP.C5,NewGuineaSingingDog,GermanShepherdDog,andZhokhov9500BPCGG6.

For all qpWave analyses, we used ADMIXTOOLS 2 (82, 83), with parameters allsnps=TRUE. From the qpWave distances, we formed an igraph object through the igraph package v.1.4.3 (<https://github.com/igraph>) and performed hierarchical clustering with pheatmap v.1.0.12 in R.

f-Statistics. We confirmed the unique ancestries of the two dingo clusters through symmetry f_4 -statistics of form f_4 (Curraurrang 2k, Nullarbor; *Test*, Andean Fox) where Curraurrang represents data from samples Curraurrang 2019 bp and Curraurrang 2007 bp, Nullarbor represents data from samples Nullarbor 892 bp and Nullarbor 1113 bp, and *Test* represents data from other ancient and present-day canine groups. We then assessed the relative affinity of a diversity of ancient canines to the two dingo groups through f_4 -statistics of form f_4 (Nullarbor, *Test*; Curraurrang 2k, Andean Fox) where *Test* represents ancient and present-day canine groups. The proportion of dingo ancestry in modern-day dingo genomes was calculated as the ratio between two f_4 -statistics:

$$\alpha (\text{Dingo Ancestry Proportion}) = \frac{f_4(\text{Russia_Baikal_7k, AndeanFox; Test Modern Dingoes, EnglishCockerSpaniel})}{f_4(\text{Russia_Baikal_7k, AndeanFox; Ancient Dingo Clusters, EnglishCockerSpaniel})}$$

Finally, we assessed whether present-day dingoes in addition to ancient or present-day canines, are consistent with being formed through a mixture of the two ancient dingo groups through f_3 -statistics in the form f_3 (*Test*; Curraurrang 2k, Nullarbor) where *Test* represents ancient and present-day canines. All *f*-statistics were computed with ADMIXTOOLS 2 (82, 83) with parameters allsnps=TRUE.

qpGraph. To understand the sequence of events leading up to dingo arrival into Australia, we started with the preferred model tested in Bergström et al. (38) as a scaffold to which we appended SE and NW Dingoes ancient clusters at all four

possible positions that fit the *f*-statistics tested. We used ADMIXTOOLS 2 (82, 83) package to fit the four tested topologies and compute the likelihood value for each of the models (Fig. 5).

Timing of Admixture. The two best-fitting models tested using qpGraph involved an admixture pulse between SE Dingoes and New Guinea singing dogs; we used the DATES (84) package v753 (<https://github.com/priyamoorjani/DATES>) to estimate the timing of the admixture pulse. We tested both pulse directions as populations, as well as where either the source or target is a single sample. All the tests showed consistent results (Fig. 6).

mtDNA Analyses. For those samples with $>0.01 \times$ average depth-of-coverage in our nuclear genomic analyses, we extracted the pileup of reads aligned to the mitochondrion scaffold of the canFam3.1 assembly. Data for the remaining ancient dingo samples were processed separately. Raw sequencing reads were demultiplexed using "sabre" (<http://github.com/najoshi/sabre>) according to their unique 7-mer barcode combinations. Using AdapterRemoval (70) v2.1.2 we trimmed residual adapters and low-quality bases ($<$ Phred20 -minquality 4); merged overlapping paired-end reads (minimum overlap = 11 nt); and discarded merged reads $<$ 30 bp (-minlength 30). Read quality was visualized using fastQC v0.10.1 (<https://www.bioinformatics.babraham.ac.uk/projects/fastqc/>) before and after trimming to make sure the trimming was efficient. Merged reads for each sample were mapped to the mitochondrion scaffold of the canFam3.1 assembly using BWA (85) v0.7.8 (aln -t 8 -l 1024 -n 0.04 -o 2). Reads with a mapping quality Phred score $>$ 30 were selected and retained using the SAMtools (86) v1.4 view command (-q 30), and duplicate reads were discarded using "FilterUniqueSAMCons.py" (87).

Samples with fewer than 1,000 unique reads mapped to the mitochondrial reference were excluded from further analysis, as were any sequences from putatively ancient specimens of unknown age (i.e., for which no radiocarbon date was available). A final 75% majority consensus sequence was then generated for each of the remaining samples ($n = 30$) using Geneious v10.2.6 (<https://www.geneious.com>), calling nucleotides only for sites with a minimum depth-of-coverage of $2 \times$. We used the MUSCLE (88) algorithm, as implemented in Geneious, to align the consensus sequences generated in this step with previously published sequences downloaded from GenBank. We then used PopART (89) to create a median-joining haplotype network (90) from this alignment, which comprised sequences from 16 ancient dingoes, 40 modern dingoes, three New Guinea singing dogs, and three other domestic dogs with closely related haplotypes.

We used BEAST2 (91) v2.7.3 to generate a time-scaled phylogeny from our mitochondrial sequence alignment. In preliminary experiments, we attempted to use only the age of our radiocarbon-dated ancient dingo sequences to calibrate our phylogeny and estimate the substitution rate; however, a date randomization test and leave-one-out cross-validation tests indicated that the temporal information encompassed by these ages did not provide sufficient power to estimate the substitution rate. Consequently, we placed an informative prior distribution on the substitution rate (normal distribution with a mean of 8.1941×10^{-8} and SD of 5.3×10^{-9}) based on the results presented by Zhang et al. (44). Our final BEAST2 analyses used a Coalescent Constant Size tree prior and Optimised Relaxed Clock model. We used the

TN93 substitution model, which was the best-fitting model according to the Bayesian Information Criterion in ModelFinder (92) as implemented in IQTREE (93) v1.6.2.

We ran three Markov chain Monte Carlo chains for 10,000,000 generations and took a sample of 10,000 states from each chain. Convergence of parameter values between the three chains and combined effective sample sizes $>$ 200 were assessed using Tracer (94) v1.7.2. The first 10% of samples from each chain were discarded as burn-in, and we combined the remainder using LogCombiner (91) v2.7.3. A total of 27,000 trees were summarized using TreeAnnotator (91) v2.7.3

to create a maximum clade credibility tree with mean TMRCA (calculated only for branches with posterior probability ≥ 0.9).

Data, Materials, and Software Availability. The DNA sequencing reads generated for this study have been deposited in the European Nucleotide Archive (ENA) (PRJEB75610) (95). Mitochondrial genome consensus sequences constructed from these data are available on GenBank (PP812314-PP812321 & PP812323-PP812333) (96). Genotype files and other supplementary data are available on Figshare (DOI: 10.25909/25885747) (97).

ACKNOWLEDGMENTS. We acknowledge the traditional custodians of the lands from which specimens used in this study have been collected and pay our respects to Elders, past, and present. Special thanks to Clem Lawrie, Senior Murring Custodian, and Native Title Holder for facilitating access to dingo specimens from Koonalda Cave. We also acknowledge the La Pouse Local Land Council and Metropolitan Local Aboriginal Land Council for granting permission to radiocarbon date and genetically analyze dingo specimens from archaeological sites in NSW. We extend our sincere appreciation to the following individuals for their invaluable advice and assistance: Steve Johnson, Shing Kwong, Raphael Eisenhofer, Steven Bourne, Jessie Treloar, Mary-Anne Binnie, Michael Curry, Adara Curry, Brett Dalziel, Alan Treloar, Isabella Donato, Michael Westaway, Christian Huber, Pontus Skoglund, and Anders Bergström. The ARCHE at Griffith University and the ACAD at University of Adelaide provided access to ancient DNA laboratories. We extend gratitude to the staff at the Australian Museum—including Val Attenbrow, Allison Dejanovic, Niamh Formosa, Dale Higginson, Rebecca Jones, and Mariko Smith—for granting access to collections and museum study permits. We appreciate the South Australian Museum, QLD Museum, and Western Australian Museum for granting access to specimens in their collections. We thank QLD Parks and Wildlife Service and the Department of Environment and Science (QLD) for providing access to K'gari dingo specimens, and National Parks and Wildlife South Australia for assistance with field logistics and permitting. We are grateful to Australian Speleological Federation members—including Nicholas White, Susan White, Margaret James, Daryl Carr, Denis Marsh, Greg Leeder, Ian Curtis, and Steve Milner—who coordinated and conducted fieldwork on the Nullarbor. Additionally, we thank the AGRF, Garvan Institute of Medical Research, Macrogen, and Novogene Bioinformatics Technology Corporation Limited for providing high-throughput DNA sequencing services. Finally, we extend our gratitude to two anonymous reviewers,

whose comments improved this manuscript. This work was supported by the Environmental Futures Research Institute Strategic Leverage Fund, Griffith University; the Australian Research Council Centre of Excellence for Australian Biodiversity and Heritage (ARC CE170100015); an Australian Research Council Laureate Fellowship (ARC FL140100260); and an Australian Research Council Discovery Project award (DP210101960). ER acknowledges support for Nullarbor fieldwork and radiocarbon dating from a Barbara Kidman Fellowship and funding from the Environment Institute, University of Adelaide.

Author affiliations: ^aAustralian Centre for Ancient DNA, School of Biological Sciences, The University of Adelaide, Adelaide, SA 5005, Australia; ^bThe Environment Institute, School of Biological Sciences, The University of Adelaide, Adelaide, SA 5005, Australia; ^cAncient DNA Facility, Defence Genomics, Genomics Research Centre, Queensland University of Technology, Kelvin Grove, QLD 4059, Australia; ^dInnovation Division, Forensic Science Queensland, Queensland Health, Coopers Plains, QLD 4108, Australia; ^eDepartment of Biology, The Pennsylvania State University, State College, PA 16802; ^fSchool of Science, Technology and Engineering, University of the Sunshine Coast, Maroochydore, QLD 4556, Australia; ^gCentre for Bioinnovation, University of the Sunshine Coast, Maroochydore, QLD 4556, Australia; ^hCentre for Planetary Health and Food Security, School of Environment and Science, Griffith University, Nathan, QLD 4111, Australia; ⁱFundación Agencia Aragonesa para la Investigación y el Desarrollo (ARAID), Zaragoza 50018, Spain; ^jInstituto Universitario de Investigación en Ciencias Ambientales de Aragón (IUCA)-Grupo Aragosaurus, Universidad de Zaragoza, Zaragoza 50009, Spain; ^kGrützner Laboratory of Comparative Genomics, School of Biological Sciences, The University of Adelaide, Adelaide, SA 5005, Australia; ^lAustralian Research Council Centre of Excellence for Australian Biodiversity and Heritage (CABAH), Adelaide SA 5005, Australia; ^mNational Centre for Indigenous Genomics, John Curtin School of Medical Research, Australian National University, Acton ACT 2601, Australia; ⁿIndigenous Genomics, Telethon Kids Institute, Adelaide, SA 5000, Australia; ^oEarth and Sustainability Science Research Centre, School of Biological, Earth & Environmental Sciences, University of New South Wales Sydney, Sydney NSW 2052, Australia; ^pSchool of Biosciences, University of Melbourne, Royal Parade, Parkville, VIC 3052, Australia; ^qEcology and Evolutionary Biology, School of Biological Sciences, The University of Adelaide, Adelaide SA 5005, Australia; ^rEvolution of Cultural Diversity Initiative, School of Culture, History and Language, College of Asia and the Pacific, The Australian National University, Acton, ACT 2601, Australia; ^sArchaeology and Natural History, School of Culture, History and Language, College of Asia and the Pacific, Australian National University, Acton, ACT 2601, Australia; ^tAustralian Museum Research Institute, Australian Museum, Sydney, NSW 2010, Australia; ^uAustralian Research Council Centre of Excellence for Australian Biodiversity and Heritage, The Australian National University, Acton, ACT 2601, Australia; ^vSchool of Anthropology and Archaeology, University of Auckland, Auckland 1010, New Zealand; ^wQueensland Department of Education, Kelvin Grove State College, Kelvin Grove, QLD 4059, Australia; ^xSchool of Social Sciences, University of Western Australia, Crawley, WA 6009, Australia; ^yGulbali Institute, Charles Sturt University, Albury, NSW 2640, Australia; and ^zManaaki Whenua—Landcare Research, Lincoln, Canterbury 7608, New Zealand

1. L. K. Corbett, Morphological comparisons of Australian and Thai dingoes: A reappraisal of dingo status, distribution and ancestry. *Proc. Ecol. Soc. Aust.* **12**, 277–291 (1985).
2. M. A. Filiios, P. S. C. Taçon, Who let the dogs in? A review of the recent genetic evidence for the introduction of the dingo to Australia and implications for the movement of people. *J. Archaeol. Sci. Rep.* **7**, 782–792 (2016).
3. A. Bergström *et al.*, Origins and genetic legacy of prehistoric dogs. *Science* **370**, 557–564 (2020).
4. K. M. Cairns, A. N. Wilton, New insights on the history of canids in Oceania based on mitochondrial and nuclear data. *Genetica* **144**, 553–565 (2016).
5. S.-J. Zhang *et al.*, Genomic regions under selection in the feralization of the dingoes. *Nat. Commun.* **11**, 671 (2020).
6. K. M. Cairns, What is a dingo—origins, hybridisation and identity. *Aust. Zool.* **41**, 322–337 (2021).
7. S. Surbakti *et al.*, New Guinea highland wild dogs are the original New Guinea singing dogs. *Proc. Natl. Acad. Sci. U.S.A.* **117**, 24369–24376 (2020).
8. M. A. Field *et al.*, The Australian dingo is an early offshoot of modern breed dogs. *Sci. Adv.* **8**, eabm5944 (2022).
9. B. P. Smith *et al.*, Taxonomic status of the Australian dingo: The case for *Canis dingo* Meyer, 1793. *Zootaxa* **4564**, zootaxa.4564.1.6 (2019).
10. S. M. Jackson *et al.*, The Dogma of Dingoes—Taxonomic status of the dingo: A reply to Smith *et al.* *Zootaxa* **4564**, 198–212 (2019).
11. J. W. O. Ballard *et al.*, The Australasian dingo archetype: De novo chromosome-length genome assembly, DNA methylome, and cranial morphology. *Gigascience* **12**, giad018 (2023).
12. C. N. Johnson, S. Wroe, Causes of extinction of vertebrates during the Holocene of mainland Australia: Arrival of the dingo, or human impact? *Holocene* **13**, 941 (2003).
13. W. J. Ripple *et al.*, Status and ecological effects of the World's largest carnivores. *Science* **343**, 1241484 (2014).
14. G. Castle, M. S. Kennedy, B. L. Allen, Stuck in the mud: Persistent failure of "the science" to provide reliable information on the ecological roles of Australian dingoes. *Biol. Conserv.* **285**, 110234 (2023).
15. B. P. Smith, C. A. Litchfield, A review of the relationship between indigenous Australians, dingoes (Canis dingo) and domestic dogs (Canis familiaris). *Anthrozoös* **22**, 111–128 (2009).
16. B. Smith, *The Dingo Debate* (CSIRO Publishing, 2015).
17. L. G. Koungoulos, J. Balme, S. O'Connor, Dingoes, companions in life and death: The significance of archaeological canine burial practices in Australia. *PLoS One* **18**, e0286576 (2023).
18. J. W. O. Ballard, L. A. B. Wilson, The Australian dingo: Untamed or feral? *Front. Zool.* **16**, 1–19 (2019).
19. B. L. Allen, L. R. Allen, G. Ballard, M. Drouilly, Animal welfare considerations for using large carnivores and guardian dogs as vertebrate biocontrol tools against other animals. *Biol. Conserv.* **232**, 258–270 (2019).
20. L. Koungoulos, *The Natural And Cultural History Of The Dingo: A 3D Geometric Morphometric Investigation* (The University of Sydney, 2021).
21. L. Koungoulos, Old dogs, new tricks: 3D geometric analysis of cranial morphology supports ancient population substructure in the Australian dingo. *Zoomorphology* **139**, 263–275 (2020).
22. K. M. Cairns, M. S. Crowther, H. G. Parker, E. A. Ostrander, M. Letnic, Genome-wide variant analyses reveal new patterns of admixture and population structure in Australian dingoes. *Mol. Ecol.* **32**, 4133–4150 (2023).
23. J. Koler-Matznick, I. Lehr Brisbin, M. Feinstein, S. Bulmer, An updated description of the New Guinea singing dog (*Canis hallstromi*, Troughton 1957). *J. Zool.* **261**, 109–118 (2003).
24. P. Savolainen, T. Leitner, A. N. Wilton, E. Matisoo-Smith, J. Lundeberg, A detailed picture of the origin of the Australian dingo, obtained from the study of mitochondrial DNA. *Proc. Natl. Acad. Sci. U.S.A.* **101**, 12387–12390 (2004).
25. K. M. Cairns, L. M. Shannon, J. Koler-Matznick, J. W. O. Ballard, A. R. Boyko, Elucidating biogeographical patterns in Australian native canids using genome wide SNPs. *PLoS One* **13**, e0198754 (2018).
26. K. M. Cairns, S. K. Brown, B. N. Sacks, J. W. O. Ballard, Conservation implications for dingoes from the maternal and paternal genome: Multiple populations, dog introgression, and demography. *Ecol. Evol.* **7**, 9787–9807 (2017).
27. B. Allen, L. Allen, G. Ballard, S. Jackson, P. Fleming, A. Roadmap to meaningful dingo conservation. *Canid Biol. Conserv.* **20**, 45–56 (2017).
28. D. Stephens, *The Molecular Ecology of Australian Wild Dogs: Hybridization, Gene Flow and Genetic Structure at Multiple Geographic Scales* (The University of Western Australia, 2011).
29. A. N. Wilton, D. J. Steward, K. Zafiris, Microsatellite variation in the Australian dingo. *J. Hered.* **90**, 108–111 (1999).
30. D. Stephens, A. N. Wilton, P. J. S. Fleming, O. Berry, Death by sex in an Australian icon: A continent-wide survey reveals extensive hybridization between dingoes and domestic dogs. *Mol. Ecol.* **24**, 5643–5656 (2015).
31. K. M. Cairns, M. S. Crowther, B. Nesbitt, M. Letnic, The myth of wild dogs in Australia: Are there any out there? *Aust. Mammal.* **44**, 67–75 (2021).
32. K. M. Cairns, B. J. Nesbitt, S. W. Laffan, M. Letnic, M. S. Crowther, Geographic hot spots of dingo genetic ancestry in southeastern Australia despite hybridisation with domestic dogs. *Conserv. Genet.* **21**, 77–90 (2020).
33. S. Wasef *et al.*, Insights into aboriginal Australian mortuary practices: Perspectives from ancient DNA. *Front. Ecol. Evol.* **8**, 217 (2020), 10.3389/fevo.2020.00217.
34. B. Llamas *et al.*, Late pleistocene Australian marsupial DNA clarifies the affinities of extinct megafaunal kangaroos and wallabies. *Mol. Biol. Evol.* **32**, 574–584 (2014).

35. L. C. White, K. J. Mitchell, J. J. Austin, Ancient mitochondrial genomes reveal the demographic history and phylogeography of the extinct, enigmatic thylacine (*Thylacinus cynocephalus*). *J. Biogeogr.* **45**, 1–13 (2018).
36. J. L. Wright *et al.*, Ancient nuclear genomes enable repatriation of Indigenous human remains. *Sci. Adv.* **4**, eaau5064 (2018).
37. J. Plassais *et al.*, Whole genome sequencing of canids reveals genomic regions under selection and variants influencing morphology. *Nat. Commun.* **10**, 1489 (2019).
38. A. Bergström *et al.*, Grey wolf genomic history reveals a dual ancestry of dogs. *Nature* **607**, 313–320 (2022).
39. A. H. Freedman *et al.*, Genome sequencing highlights the dynamic early history of dogs. *PLoS Genet.* **10**, e1004016 (2014).
40. M. P. Williams, P. Flegontov, R. Maier, C. D. Huber, Testing times: Challenges in disentangling admixture histories in recent and complex demographics. bioRxiv [Preprint] (2023). <https://doi.org/10.1101/2023.11.13.566841> (Accessed 24 January 2024).
41. B. M. Peter, Admixture, population structure, and F-statistics. *Genetics* **202**, 1485–1501 (2016).
42. A. N. Wilton, "DNA methods of assessing dingo purity" in *A Symposium on the Dingo*, D. L. C. R. Dickman, Ed. (Royal Zoological Society of New South Wales, 2001).
43. A. E. Elledge, L. R. Allen, B.-L. Carlsson, A. N. Wilton, L.K.-P. Leung, An evaluation of genetic analyses, skull morphology and visual appearance for assessing dingo purity: Implications for dingo conservation. *Wildl. Res.* **35**, 812–820 (2008).
44. M. Zhang *et al.*, Ancient DNA evidence from China reveals the expansion of Pacific dogs. *Mol. Biol. Evol.* **37**, 1462–1469 (2020).
45. M. C. R. Oskarsson *et al.*, Mitochondrial DNA data indicate an introduction through Mainland Southeast Asia for Australian dingoes and Polynesian domestic dogs. *Proc. R. Soc. B Biol. Sci.* **279**, 967–974 (2011).
46. L. Dayton, On the trail of the first Dingo. *Science* **302**, 555–556 (2003).
47. S. Wasef *et al.*, A contextualised review of genomic evidence for gene flow events between Papuans and Indigenous Australians in Cape York. *QLD Quat. Int.* **603**, 22–30 (2021).
48. A. Barham, "Late Holocene maritime societies in the Torres Strait Islands, northern Australia—Cultural arrival or cultural emergence?" in *East of Wallace's Line: Studies of Past and Present Maritime Cultures of the Indo-Pacific Region*, S. O'Connor, P. Veth, Eds. (A.A. Balkema, Rotterdam, 2000).
49. S. Greer, R. Henry, S. McIntyre-Tamwoy, Mainland magic: Interpreting cultural influences across Cape York-Torres Strait. *Quat. Int.* **385**, 69–78 (2015).
50. F. D. McCarthy, "The use of stone tools to map patterns of diffusion" in *Stone Tools as Cultural Markers: Change Evolution and Complexity*, R.V.S. Wright, Ed. (Australian Institute of Aboriginal Studies, Canberra, 1977), pp. 250–262.
51. M. J. Rowland, The distribution of Aboriginal watercraft on the east coast of Queensland: Implications for culture contact. *Aus. Aborig. Stud.* **1987**, 38–45 (2020).
52. A. B. J. Lambrides *et al.*, Changing use of Lizard Island over the past 4000 years and implications for understanding Indigenous offshore island use on the Great Barrier Reef. *QLD Archaeol. Res.* **23**, 43–109 (2020).
53. G. C. Conroy *et al.*, Conservation concerns associated with low genetic diversity for K'gari-Fraser Island dingoes. *Sci. Rep.* **11**, 1–10 (2021).
54. S. Carlhoff *et al.*, Genome of a middle Holocene hunter-gatherer from Wallacea. *Nature* **596**, 543–547 (2021).
55. R. Appleby, J. Mackie, B. Smith, L. Bernede, D. Jones, Human-dingo interactions on Fraser Island: An analysis of serious incident reports. *Aust. Mammal.* **40**, 146–156 (2017).
56. G. Conroy, S. Ogbourne, R. W. Lamont, "A baseline genetic analysis of the K'gari-Fraser Island dingo population" (University of the Sunshine Coast, Queensland, Australia, 2017).
57. S. Gopalakrishnan *et al.*, Interspecific gene flow shaped the evolution of the genus *Canis*. *Curr. Biol.* **28**, 3441–3449.e5 (2018).
58. L. A. F. Frantz *et al.*, Genomic and archaeological evidence suggest a dual origin of domestic dogs. *Science* **352**, 1228–1231 (2016).
59. M.-H.S. Sinding *et al.*, Arctic-adapted dogs emerged at the Pleistocene-Holocene transition. *Science* **368**, 1495–1499 (2020).
60. M. Ni Leathlobhair *et al.*, The evolutionary history of dogs in the Americas. *Science* **361**, 81–85 (2018).
61. L. R. Botigué *et al.*, Ancient European dog genomes reveal continuity since the Early Neolithic. *Nat. Commun.* **8**, 1–11 (2017).
62. J. Ramos-Madrugal *et al.*, Genomes of Pleistocene Siberian wolves uncover multiple extinct wolf lineages. *Curr. Biol.* **31**, 198–206.e8 (2021).
63. C. B. Ramsey, Radiocarbon calibration and analysis of stratigraphy: The OxCal program. *Radiocarbon* **37**, 425–430 (1995).
64. A. G. Hogg *et al.*, SHCal20 southern hemisphere calibration, 0–55,000 years cal BP. *Radiocarbon* **62**, 759–778 (2020).
65. M. Meyer, M. Kircher, Illumina sequencing library preparation for highly multiplexed target capture and sequencing. *Cold Spring Harb. Protoc.* 2010, db.prot5448 (2010).
66. N. Rohland, E. Harney, S. Mallick, S. Nordenfelt, D. Reich, Partial uracil-DNA-glycosylase treatment for screening of ancient DNA. *Philos. Trans. R. Soc. Lond. B Biol. Sci.* **370**, 20130624 (2015).
67. K. J. Mitchell *et al.*, Ancient mitochondrial DNA reveals convergent evolution of giant short-faced bears (Tremarctinae) in North and South America. *Biol. Lett.* **12**, 20160062 (2016).
68. J. A. F. Yates *et al.*, Reproducible, portable, and efficient ancient genome reconstruction with nf-core/eager. *PeerJ* **16**, e10947 (2020).
69. P. Di Tommaso *et al.*, Nextflow enables reproducible computational workflows. *Nat. Biotechnol.* **35**, 316–319 (2017).
70. M. Schubert, S. Lindgreen, L. Orlando, AdapterRemoval v2: Rapid adapter trimming, identification, and read merging. *BMC Res. Notes* **9**, 88 (2016).
71. A. Oliva, R. Tobler, A. Cooper, B. Llamas, Y. Souilmi, Systematic benchmark of ancient DNA read mapping. *Brief. Bioinform.* **22**, bbab076 (2021).
72. G. Jun, M. K. Wing, G. R. Abecasis, H. M. Kang, An efficient and scalable analysis framework for variant extraction and refinement from population-scale DNA sequence data. *Genome Res.* **25**, 918–925 (2015).
73. J. Neukamm, A. Peltzer, K. Nieselt, DamageProfiler: Fast damage pattern calculation for ancient DNA. *Bioinformatics* **37**, 3652–3653 (2020).
74. T. S. Korneliusen, A. Albrechtsen, R. Nielsen, ANGSD: Analysis of next generation sequencing data. *BMC Bioinformatics* **15**, 356 (2014).
75. S. Chen, Y. Zhou, Y. Chen, J. Gu, fastp: An ultra-fast all-in-one FASTQ preprocessor. *Bioinformatics* **34**, i884–i890 (2018).
76. T. C. Lamnidis *et al.*, Ancient Fennoscandian genomes reveal origin and spread of Siberian ancestry in Europe. *Nat. Commun.* **9**, 5018 (2018).
77. K. Okonechnikov, A. Conesa, F. Garcia-Alcalde, Qualimap 2: Advanced multi-sample quality control for high-throughput sequencing data. *Bioinformatics* **32**, 292–294 (2016).
78. N. Patterson, A. L. Price, D. Reich, Population structure and eigenanalysis. *PLoS Genet.* **2**, e190 (2006).
79. A. L. Price *et al.*, Principal components analysis corrects for stratification in genome-wide association studies. *Nat. Genet.* **38**, 904–909 (2006).
80. H. Wickham, *ggplot2: Elegant Graphics for Data Analysis* (Springer Science & Business Media, 2009).
81. R Core Team, *R: A Language and Environment for Statistical Computing* (R Foundation for Statistical Computing, Vienna, Austria, 2021).
82. N. Patterson *et al.*, Ancient admixture in human history. *Genetics* **192**, 1065–1093 (2012).
83. R. Maier *et al.*, On the limits of fitting complex models of population history to f-statistics. *Elife* **12**, e85492 (2023).
84. V. M. Narasimhan *et al.*, The formation of human populations in South and Central Asia. *Science* **365**, eaat7487 (2019).
85. H. Li, R. Durbin, Fast and accurate short read alignment with Burrows-Wheeler transform. *Bioinformatics* **25**, 1754–1760 (2009).
86. H. Li *et al.*, The sequence alignment/map format and SAMtools. *Bioinformatics* **25**, 2078–2079 (2009).
87. M. Kircher, Analysis of high-throughput ancient DNA sequencing data. *Methods Mol. Biol.* **840**, 197–228 (2012).
88. R. C. Edgar, MUSCLE: Multiple sequence alignment with high accuracy and high throughput. *Nucleic Acids Res.* **32**, 1792–1797 (2004).
89. J. W. Leigh, D. Bryant, Popart: Full-feature software for haplotype network construction. *Methods Ecol. Evol.* **6**, 1110–1116 (2015).
90. H. J. Bandelt, P. Forster, A. Röhl, Median-joining networks for inferring intraspecific phylogenies. *Mol. Biol. Evol.* **16**, 37–48 (1999).
91. R. Bouckaert *et al.*, BEAST 2: A software platform for Bayesian evolutionary analysis. *PLoS Comput. Biol.* **10**, e1003537 (2014).
92. S. Kalyanamoorthy, B. Q. Minh, T. K. F. Wong, A. von Haeseler, L. S. Jermini, ModelFinder: Fast model selection for accurate phylogenetic estimates. *Nat. Methods* **14**, 587–589 (2017).
93. L.-T. Nguyen, H. A. Schmidt, A. von Haeseler, B. Q. Minh, IQ-TREE: A fast and effective stochastic algorithm for estimating maximum-likelihood phylogenies. *Mol. Biol. Evol.* **32**, 268–274 (2015).
94. A. Rambaut, A. J. Drummond, D. Xie, G. Baele, M. A. Suchard, Posterior summarization in bayesian phylogenetics using tracer 1.7. *Syst. Biol.* **67**, 901–904 (2018).
95. Y. Souilmi *et al.*, Deposited sequencing data. European Read Archive. <https://www.ebi.ac.uk/enal/browser/view/PRJEB75610>. Deposited 12 May 2024.
96. Y. Souilmi *et al.*, Deposited mitochondrial consensus sequences (PP812314-PP812321 & PP812323-PP812333). GeneBank. <https://www.ncbi.nlm.nih.gov/nuccore/PP812314> <https://www.ncbi.nlm.nih.gov/nuccore/PP812315> <https://www.ncbi.nlm.nih.gov/nuccore/PP812317> <https://www.ncbi.nlm.nih.gov/nuccore/PP812318> <https://www.ncbi.nlm.nih.gov/nuccore/PP812319> <https://www.ncbi.nlm.nih.gov/nuccore/PP812320> <https://www.ncbi.nlm.nih.gov/nuccore/PP812321> <https://www.ncbi.nlm.nih.gov/nuccore/PP812322> <https://www.ncbi.nlm.nih.gov/nuccore/PP812323> <https://www.ncbi.nlm.nih.gov/nuccore/PP812324> <https://www.ncbi.nlm.nih.gov/nuccore/PP812325> <https://www.ncbi.nlm.nih.gov/nuccore/PP812327> <https://www.ncbi.nlm.nih.gov/nuccore/PP812328> <https://www.ncbi.nlm.nih.gov/nuccore/PP812329> <https://www.ncbi.nlm.nih.gov/nuccore/PP812330> <https://www.ncbi.nlm.nih.gov/nuccore/PP812331> <https://www.ncbi.nlm.nih.gov/nuccore/PP812332> <https://www.ncbi.nlm.nih.gov/nuccore/PP812333>. Deposited 15 May 2024.
97. Y. Souilmi *et al.*, Deposited genotype data and phylogenetic analysis Files. Figshare. <https://dx.doi.org/10.25909/25885747>. Deposited 15 June 2024.